

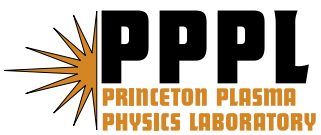
---

# Princeton Plasma Physics Laboratory

---

PPPL-

PPPL-



Prepared for the U.S. Department of Energy under Contract DE-AC02-76CH03073.

# Princeton Plasma Physics Laboratory

## Report Disclaimers

---

### Full Legal Disclaimer

This report was prepared as an account of work sponsored by an agency of the United States Government. Neither the United States Government nor any agency thereof, nor any of their employees, nor any of their contractors, subcontractors or their employees, makes any warranty, express or implied, or assumes any legal liability or responsibility for the accuracy, completeness, or any third party's use or the results of such use of any information, apparatus, product, or process disclosed, or represents that its use would not infringe privately owned rights. Reference herein to any specific commercial product, process, or service by trade name, trademark, manufacturer, or otherwise, does not necessarily constitute or imply its endorsement, recommendation, or favoring by the United States Government or any agency thereof or its contractors or subcontractors. The views and opinions of authors expressed herein do not necessarily state or reflect those of the United States Government or any agency thereof.

### Trademark Disclaimer

Reference herein to any specific commercial product, process, or service by trade name, trademark, manufacturer, or otherwise, does not necessarily constitute or imply its endorsement, recommendation, or favoring by the United States Government or any agency thereof or its contractors or subcontractors.

---

## PPPL Report Availability

### Princeton Plasma Physics Laboratory:

<http://www.pppl.gov/techreports.cfm>

### Office of Scientific and Technical Information (OSTI):

<http://www.osti.gov/bridge>

---

### Related Links:

[U.S. Department of Energy](#)

[Office of Scientific and Technical Information](#)

[Fusion Links](#)

# Interpretation of the finite pressure gradient effects in the reversed shear Alfvén eigenmode theory

N. N. Gorelenkov, G. J. Kramer, R. Nazikian

*Princeton Plasma Physics Laboratory,  
Princeton University, P.O.Box 451, 08543*

## Abstract

Ideal MHD equations employed in the NOVA code are analyzed analytically and numerically in order to investigate the role of the pressure gradient on global reversed shear Alfvén eigenmodes (RSAEs) or Alfvén cascades. We confirm both numerically and analytically conclusions obtained earlier using the ideal MHD code NOVA [1] and analytically [2] that the plasma pressure gradient plays a key role in the existence condition and in the dispersion relation for the mode. The effect of the plasma pressure gradient is to shift the mode frequency up at the low part of the RSAE frequency chirp and downshift the mode frequency when the frequency approaches the TAE gap. This finding is opposite to predictions in a recent publication [3], where the pressure gradient is found to be always stabilizing by means of downshifting the RSAE frequency and enhancing its interaction with the continuum. We resolve this discrepancy by showing that neglecting the pressure gradient effect on the plasma equilibrium (modification of the Shafranov shift and the averaged curvature) leads to conclusions at variance to the numerical and analytical results presented here. A new variational approximation of the RSAE is introduced which compares remarkably well with NOVA solutions. With this new approximation we clearly demonstrate the diagnostic potential and limitations of the RSAE frequency measurement for MHD spectroscopy.

## I. INTRODUCTION

In this paper we analyze both numerically and analytically the equations employed in the ideal MHD code NOVA [4, 5] to assess the effect of the pressure gradient on the existence condition and eigenfrequency of Alfvén cascade modes also known as reversed shear Alfvén eigenmodes (RSAEs). These modes are observed in many experiments with reversed magnetic shear [6, 7]. Their characteristics are that they are localized to the region near the minimum in the magnetic safety factor and typically chirp up in frequency as  $q_{min}$  decreases. The frequency chirp range is bounded in experiments and is given at the low frequency end,  $\omega_{min}$ , by the geodesic acoustic mode [3] together with a contribution from the pressure gradient [1] and is limited at the high frequency end by the TAE frequency  $\omega_{TAE}$  [8].

It was shown numerically [1] that the plasma pressure gradient plays a key role in the existence condition for the RSAE and results in an upshift of the RSAE frequency (at fixed  $q_{min}$ ) in the low frequency range of the chirp [20]. The pressure gradient is also responsible for a frequency downshift when the mode begins to transition to the TAE gap, i.e. near the top of RSAE frequency range. The latter case is associated with the well known stabilization of TAEs by the pressure gradient [9].

The effect of the finite pressure has been studied analytically recently and was shown to result in the upshift of the RSAE frequency, with a minimum mode frequency determined by the Geodesic Acoustic Mode (GAM) [3]. However an increase in the pressure gradient was predicted to cause a downshift of RSAE frequency and its possible stabilization due to stronger interaction with the Alfvén continuum. This result is at odds with numerical analysis presented in Ref. [1]. The reason for the discrepancy was recently identified in Ref. [2] mostly due to the averaged curvature effect. Thus, it seems essential to interpret the numerical solutions obtained in Ref. [1] by means of analytical analysis of the same system of equations used in the NOVA code as well as to study the pressure gradient effect numerically in more detail.

As part of the analysis a new variational principle solution is developed and applied to the RSAE eigenmode equation which shows better agreement with NOVA computations than previous analytic results over a wide range of plasma parameters.

In this paper we show that in realistic plasma conditions the pressure gradient can play a dominant role in the existence condition for the RSAEs. In particular it is interesting to note

that the plasma pressure gradient can compete with the effect of the GAM on determining the minimum RSAE frequency,  $\omega_{min}$ . Note that the finite pressure effect associated with the GAM is implicitly contained in the acoustic mode filtering technique developed in Ref. [10].

While working on this paper we learned that an analytic insight into the role of the curvature term in establishing mode criteria was obtained by Fu and Berk [2]. Our derivation reproduces their main results on the RSAE eigenmode equation and on the pressure gradient effects. However the basic set of ideal MHD equations we use is the one employed in NOVA code.

The paper is organized as follows. The derivation of the RSAE eigenmode equation is given in Section II. Section III is devoted to a comparison of existing approximate analytical solutions of the RSAE equation with NOVA numerical solutions. We also offer in that section a new, more accurate variational solution of this equation. Implications for MHD spectroscopy are presented in Section IV. Discussion and conclusions are presented in Section V.

## II. FORMULATION

To derive the Alfvén eigenmode type equation we introduce flux coordinates by defining the equilibrium magnetic field vector,  $\mathbf{B}$ , with nested flux surfaces

$$\mathbf{B} = g\nabla\varphi + \nabla\varphi \times \nabla\psi, \quad (1)$$

where  $2\pi\psi$  is the poloidal magnetic field flux,  $\varphi$  is the toroidal angle,  $g = B_\varphi R$ ,  $B_\varphi$  is the toroidal component of the equilibrium magnetic field, and  $R = |\nabla\varphi|^{-1} = R_0 - \Delta + r \cos\theta + O(\varepsilon^3)$  is the major radius,  $R_0$  is the major radius of the magnetic axis,  $\Delta = \Delta(r)$  is the Shafranov shift of the magnetic surface centers and  $\theta$  is the poloidal angle chosen following [11]. It is also useful to introduce a generalized toroidal angle,  $\zeta$ , in which together with the poloidal angle the magnetic field lines are straight. It is related to  $\varphi$  via the equation:

$$\zeta = \varphi - q\delta(r, \theta),$$

where  $\delta$  is resolved from

$$q(1 + \partial\delta(r, \theta)/\partial\theta) = g\mathcal{J}/R^2\psi',$$

and  $\mathcal{J}$  is the Jacobian. Together with equilibrium relations from Appendix A we find that  $\delta = -(\varepsilon + \Delta') \sin \theta$  in large aspect ratio plasmas in which  $\varepsilon = r/a \ll 1$  is assumed, where  $r$  is the minor radius of the magnetic surfaces and  $r = a$  at the last plasma surface. The other definitions of equilibrium quantities are given in rationalized MKS units in Appendix A together with their approximations for the case of low aspect ratio plasma and equal poloidal arc choice of the poloidal angle.

The system of four general ideal MHD equations is derived in [4, 5] from standard linearized ideal MHD equations, where four unknown variables are two components of the plasma displacement vector,  $\vec{\xi}$  (namely  $\xi_\psi = \vec{\xi} \cdot \nabla \psi$ ,  $\xi_s \equiv \vec{\xi} \cdot [\mathbf{B} \times \nabla \psi] / |\nabla \psi|^2$ ),  $\delta p_1 \equiv \mathbf{B} \cdot \delta \mathbf{B} + \delta p$  and  $\nabla \cdot \vec{\xi}$ , with  $\delta p$  being the plasma pressure perturbation and  $\delta \mathbf{B}$  being the perturbed magnetic field vector. It is important to evaluate the effect of the pressure gradient for the case where the ratio of specific heat  $\gamma = 0$ , in order to avoid effects of the beta induced gap (BAE gap [10]) or GAM (geodesic acoustic mode [3]). In the case of  $\gamma = 0$ , as can be seen from Eqs.(3.51-3.54) of Ref.[5], the fourth variable  $\nabla \cdot \vec{\xi}$  is decoupled from first three equations, which corresponds to the filtering out the sound waves, and  $\nabla \cdot \vec{\xi}$  can be resolved from Eq.(3.54) of Ref.[5]. The effect of finite  $\gamma$  is shown to introduce the beta induced gap (BAE) and also shifts the whole Alfvén spectrum up in frequency [10]. It was brought up in Ref.[3] as the only favorable pressure driven ingredient contributing to the formation of the minimum of the RSAE frequency and was related to the GAM solution near the  $q_{min}$  surface.

In the following derivation we do not required  $\delta p_1 = 0$ , leading to the coupling of Eqs.(3.51) and (3.53) in Ref.[5]. In contrast to standard derivations, we eliminate  $\delta p_1$  by multiplying Eq.(3.51) by  $(-k_s + B^{-2} [\mathbf{B} \times \nabla \psi] \cdot \nabla)$ , Eq.(3.53) by  $(-k_\psi + \nabla \psi \cdot \nabla)$  and summing them, so that the resulting equation reads:

$$\begin{aligned}
& (\nabla \psi \cdot \nabla - k_\psi) \frac{|\nabla \psi|^2}{B^2} L_{\parallel}^* \xi_s + \left( k_s - \frac{\mathbf{B} \times \nabla \psi}{B^2} \cdot \nabla \right) L_{\parallel} \xi_\psi - L_p \delta p_1 + \\
& \left( k_s - \frac{\mathbf{B} \times \nabla \psi}{B^2} \cdot \nabla \right) \left[ \frac{k_\psi}{\psi'} P' + (\mathbf{B} \cdot \mathbf{J} - |\nabla \psi|^2 S) \frac{|\nabla \psi|^2}{B^2} S \right] \xi_\psi + \\
& \left( k_s - \frac{\mathbf{B} \times \nabla \psi}{B^2} \cdot \nabla \right) (|\nabla \psi|^2 S - \mathbf{B} \cdot \mathbf{J}) \frac{|\nabla \psi|^2}{B^2} \mathbf{B} \cdot \nabla \xi_s - \\
& (\nabla \psi \cdot \nabla - k_\psi) \left[ -\frac{k_s}{\psi'} P' + \mathbf{B} \cdot \nabla \left( \frac{|\nabla \psi|^2}{B^2} S \right) + \frac{|\nabla \psi|^2 S - \mathbf{B} \cdot \mathbf{J}}{B^2} \mathbf{B} \cdot \nabla \right] \xi_\psi = 0 \quad (2)
\end{aligned}$$

where  $L_{\parallel} \equiv \omega^2 \rho + |\nabla \psi|^2 (\mathbf{B} \cdot \nabla) |\nabla \psi|^{-2} \mathbf{B} \cdot \nabla$ ,  $L_{\parallel}^* \equiv \omega^2 \rho + B^2 |\nabla \psi|^{-2} (\mathbf{B} \cdot \nabla) B^{-2} |\nabla \psi|^2 \mathbf{B} \cdot \nabla$ ,

$\mathbf{J}$  is the vector of the equilibrium plasma current,

$$L_p = (\nabla\psi \cdot \nabla - k_\psi) \left( \frac{[\mathbf{B} \times \nabla\psi] \cdot \nabla}{B^2} - k_s \right) - \left( \frac{[\mathbf{B} \times \nabla\psi] \cdot \nabla}{B^2} - k_s \right) (\nabla\psi \cdot \nabla - k_\psi) \quad (3)$$

and the rest of definitions are given in Appendix A. Strictly speaking the  $\delta p_1$  term can be eliminated only for high- $n$  modes or for cylindrical plasma, in which case Eqs.(3.52) of Ref. [5] should also be invoked.

Equation 2 contains three unknown variables and should be supplemented by Eqs.(3.51-53) of Ref. [5] for exact solution which couples shear and compressional waves. To decouple the shear branch we make use of the electrostatic potential,  $\phi$ , with the gauge  $A_\perp = 0$ , so that

$$\vec{\xi}_\perp = \frac{ic}{\omega} \frac{\mathbf{B} \times \nabla\phi}{B^2}. \quad (4)$$

From here two components of the plasma displacement are readily expressed

$$\begin{aligned} \xi_s &= \frac{ic}{\omega} \frac{\nabla\psi}{|\nabla\psi|^2} \cdot \nabla\phi, \\ \xi_\psi &= -\frac{ic}{\omega} \frac{\mathbf{B} \times \nabla\psi}{B^2} \cdot \nabla\phi. \end{aligned} \quad (5)$$

Substituting this into Eq.(2) we find

$$\begin{aligned} &(\nabla\psi \cdot \nabla - k_\psi) \frac{|\nabla\psi|^2}{B^2} L_\parallel^* \frac{\nabla\psi}{|\nabla\psi|^2} \cdot \nabla\phi - \left( k_s - \frac{\mathbf{B} \times \nabla\psi}{B^2} \cdot \nabla \right) L_\parallel \frac{\mathbf{B} \times \nabla\psi}{B^2} \cdot \nabla\phi + \frac{i\omega}{c} L_p \delta p - \\ &\quad \left( k_s - \frac{\mathbf{B} \times \nabla\psi}{B^2} \cdot \nabla \right) \left[ \frac{k_\psi}{\psi'} P' + (\mathbf{B} \cdot \mathbf{J} - |\nabla\psi|^2 S) \frac{|\nabla\psi|^2}{B^2} S \right] \frac{\mathbf{B} \times \nabla\psi}{B^2} \cdot \nabla\phi + \\ &\quad \left( k_s - \frac{\mathbf{B} \times \nabla\psi}{B^2} \cdot \nabla \right) (|\nabla\psi|^2 S - \mathbf{B} \cdot \mathbf{J}) \frac{|\nabla\psi|^2}{B^2} \mathbf{B} \cdot \nabla \left( \frac{\nabla\psi}{|\nabla\psi|^2} \cdot \nabla\phi \right) + (\nabla\psi \cdot \nabla - k_\psi) \cdot \\ &\quad \left[ -\frac{k_s}{\psi'} P' + \mathbf{B} \cdot \nabla \left( \frac{|\nabla\psi|^2}{B^2} S \right) + \frac{|\nabla\psi|^2 S - \mathbf{B} \cdot \mathbf{J}}{B^2} \mathbf{B} \cdot \nabla \right] \frac{\mathbf{B} \times \nabla\psi}{B^2} \cdot \nabla\phi = (6) \end{aligned}$$

Eq.(6) is the most general equation for the shear Alfvén modes with the only assumption given by Eq.(4).

To proceed further we take the high- $m$  (high- $n$ ) limit and assume radially localized solution, which means that  $L_p = O(m^{-1})$ , which helps to simplify Eq.(6). We then obtain

$$\begin{aligned} &\left[ \nabla\psi \cdot \nabla \frac{|\nabla\psi|^2}{B^2} L_\parallel^* \frac{\nabla\psi}{|\nabla\psi|^2} \cdot \nabla + \frac{\mathbf{B} \times \nabla\psi}{B^2} \cdot \nabla L_\parallel \frac{\mathbf{B} \times \nabla\psi}{B^2} \cdot \nabla \right] \phi + \\ &\quad \left[ \left( \frac{\mathbf{B} \times \nabla\psi}{B^2} \cdot \nabla \right) \frac{k_\psi}{\psi'} P' - (\nabla\psi \cdot \nabla) \frac{k_s}{\psi'} P' \right] \frac{\mathbf{B} \times \nabla\psi}{B^2} \cdot \nabla\phi + \end{aligned}$$

$$\begin{aligned}
& (\nabla\psi \cdot \nabla) \mathbf{B} \cdot \nabla \left( \frac{|\nabla\psi|^2}{B^2} S \right) \frac{\mathbf{B} \times \nabla\psi}{B^2} \cdot \nabla\phi + (\mathbf{B} \cdot \mathbf{J} - |\nabla\psi|^2 S) \times \\
& \left[ \left( \frac{\mathbf{B} \times \nabla\psi}{B^2} \cdot \nabla \right) \frac{|\nabla\psi|^2}{B^2} \left( \frac{S\mathbf{B} \times \nabla\psi}{B^2} + \frac{(\mathbf{B} \cdot \nabla) \nabla\psi}{|\nabla\psi|^2} \right) - \frac{(\nabla\psi \cdot \nabla) (\mathbf{B} \cdot \nabla) \mathbf{B} \times \nabla\psi}{B^2} \right] \nabla\phi = (\mathfrak{D})
\end{aligned}$$

We choose the following ansatz for the perturbed quantities

$$\phi = \sum_j \phi_{j-m}(r) e^{-i\omega t + ij\theta - in\zeta}, \quad (8)$$

where  $m$  is the dominant harmonic of the RSAE solution, which is known from numerical and analytical solutions [1, 12]. With the differential operators in the form described in Appendix A we further simplify Eq.(7) by multiplying it by  $e^{-im\theta} \mathcal{J}/\varepsilon |\nabla\psi|^2$  and integrating over  $\theta$ . Since the effects of  $\varepsilon$  up to  $O(\varepsilon^2)$  have already been accounted for in [12] (we refer the reader for the derivation details to that reference, but caution that our derivation is in a different equilibrium coordinate), we show the derivation by including terms due to the pressure gradient, some of which were ignored. We find three coupled equations for zero and first order poloidal harmonics, which have ordering  $\phi_0 = O(1)$ ,  $\phi_{\pm 1} = O(\varepsilon)$ :

$$(L_0^0 + L_0^2) \phi_0 + L_{0,+1}^1 \phi_{+1} + L_{0,-1}^1 \phi_{-1} = 0 \quad (9)$$

$$L_{\pm 1}^0 \phi_{\pm 1} + L_{\pm 1,0}^1 \phi_0 = 0 \quad (10)$$

where differential operators are given by

$$\begin{aligned}
L_j^0 &= (\bar{\omega}^2 - k_j^2) (\partial_r^2 - (m+j)^2), \\
L_0^2 &= \frac{\alpha m^2}{q^2} \left( \frac{3\Delta'}{2} + \frac{r\Delta''}{2} + \frac{\varepsilon}{2} - \frac{\varepsilon}{q^2} \right), \\
L_{0,\pm 1}^1 &\equiv l_{1,\pm} \pm l_{2,\pm}, \quad L_{\pm 1,0}^1 \equiv l_{1,\pm} \mp l_{2,\pm}, \\
l_{1,\pm} &= \bar{\omega}^2 (\varepsilon - \Delta') (\partial_r^2 - m^2) - \frac{3\Delta' + \varepsilon}{2} k_0 (k_{\pm 1} - k_0) \partial_r^2 - \frac{\Delta' + \varepsilon}{2} k_0 m^2 (k_{\pm 1} - k_0) - \frac{\alpha m^2}{2q^2}, \\
l_{2,\pm} &= -\frac{\Delta' + r\Delta'' + \varepsilon}{2} m (k_{\pm 1}^2 - k_0^2) \partial_r + \frac{\Delta' + r\Delta'' + \varepsilon}{2q^2} m \partial_r - \frac{\alpha m^2}{2q^2}
\end{aligned}$$

and  $\partial_r \equiv r\partial/\partial r$ . The notations we adopt are the following. The subscript  $j$  refers to the  $m+j$  poloidal harmonic of the perturbation (see Eq.(8)). The  $j$  superscript denotes the ordering of differential operators,  $L^j = O(\varepsilon^{|j|})$ . It is important to note that  $L_0^2$  is derived from the second line terms of Eq.(7) due to the magnetic field line curvature. We also

neglected the effect of the plasma density gradient for simplicity and assume it to be zero. Finally, in deriving the eigenmode equation we assumed that the mode frequency is close to the shear Alfvén continuum of the  $m$ -th harmonic, i.e.  $\bar{\omega} \simeq k_0$ , where  $\bar{\omega} = \omega R_0/v_A$ ,  $v_A$  is the Alfvén velocity.

To build the eigenmode equation we multiply Eq.(9) by  $(\partial_r^2 - m^2)$  and express unknown  $(\partial_r^2 - m^2) \phi_{\pm 1}$  using the two Eqs.(10), which result in the following

$$(L_0^0 + L_0^2) (\partial_r^2 - m^2) \phi_0 + q^2 \frac{l_{l,+}^2 + l_{1,-}^2 - l_{2,+}^2 - l_{2,-}^2 + 2k_0 q (l_{1,-}^2 - l_{1,+}^2 - l_{2,-}^2 + l_{2,+}^2)}{1 - 4k_0^2 q^2} \phi_0 = 0, \quad (11)$$

where we made use of  $n, m \gg 1$ . Collecting corresponding terms and dividing Eq.(11) by  $(\partial_r^2 - m^2)$  we find the eigenmode equation

$$L_0^0 \phi_0 + 2m^2 \bar{\omega}^2 \frac{\varepsilon (\varepsilon + 2\Delta') - \delta_{m\partial} (r\Delta'' - \Delta') (r\Delta'' + 3\Delta' + 2\varepsilon - 2\alpha)}{1 - 4k_0^2 q^2} \phi_0 + \left[ 4m^2 \bar{\omega}^2 \frac{\alpha \Delta'}{1 - 4k_0^2 q^2} - \frac{m^2}{2q^2} \frac{\alpha^2}{1 - 4k_0^2 q^2} + \frac{\alpha m^2}{q^2} \left( \frac{3\Delta'}{2} + \frac{r\Delta''}{2} + \frac{\varepsilon}{2} - \frac{\varepsilon}{q^2} \right) \right] \phi_0 = 0, \quad (12)$$

where we left terms proportional to  $(r\Delta'' - \Delta') = -4\Delta' + \varepsilon + \alpha$ ,  $\alpha \equiv -R_0 q^2 \beta'$ , (compare with [2, 12]), which are nonzero in general as one can see from Eqs.(B7,B8), and introduced a symbol  $\delta_{m\partial} = \partial_r^2 \phi_0 / (\partial_r^2 - m^2) \phi_0$ , which is approximated as equal 1 if  $\partial_r^2 \gg m^2$  and 0 if  $\partial_r^2 \ll m^2$ , i.e. the only analytically treatable cases. In fact the terms  $(r\Delta'' - \Delta')$  can be of importance especially at the threshold conditions of the mode existence when  $\partial_r^2 \gg m^2$  (in the opposite case  $m^2 \gg \partial_r^2$ , more typical for the experimental conditions, these terms are negligible and  $\delta_{m\partial} = 0$ ). In a special case of flat plasma current and parabolic pressure profile  $(r\Delta'' - \Delta') = 0$  exactly.

### A. Simplified eigenmode equation and qualitative analysis of plasma pressure gradient, $\alpha$ effect

For further analysis it is useful to expand Eq.(12) near  $q = q_{min}$  point to present it in the form analyzed in Ref.[8]. The localized solution within the ideal MHD theory is possible for the case  $k_0 > 0$ , which corresponds to  $q < m/n$  and the RSAE frequency then chirps up as  $q_{min}$  drops below  $m/n$ . It was shown that for the downchirp case ( $q > m/n$ ) and  $|\bar{\omega}| < |k_0|$  the mode can not exist [12], whereas the downchirp case with  $|\bar{\omega}| > |k_0|$  has been found and reported in numerical simulations at sufficiently large  $\alpha$  [1]. Numerical modeling shows that

RSAE in this case interact with the continuum, which may require kinetic treatment of the problem [13].

We make use of the  $q$ -profile given by Eq.(B1). Defining the new variable  $x = m(r - r_0)/r_0$  one can rewrite Eq.(12) as

$$-\partial_x (S_\omega + x^2) \partial_x \phi_0 + (S_\omega + x^2) \phi_0 = (Q_{tor} + Q_p) \phi_0 \equiv Q \phi_0, \quad (13)$$

where  $S_\omega \equiv 2(\bar{\omega} - k_0) m q_0^2 / r_0^2 q_0'' = (\bar{\omega} - k_0) m q_0 w^2 / r_0^2$ , and  $k_0$  is determined by Eq.(A4),

$$Q_{tor} = 2m \frac{\bar{\omega}_0 q_0^2 \varepsilon (\varepsilon + 2\Delta') - \delta_{m\partial} (r\Delta'' - \Delta') (3\varepsilon - \alpha)}{r_0^2 q_0'' (1 - 4k_0^2 q_0^2)}$$

$$Q_p = \frac{m\alpha}{r_0^2 q_0'' k_0} \left[ 4\bar{\omega}_0^2 q_0^2 \frac{\Delta'}{1 - 4k_0^2 q^2} - \frac{\alpha/2}{1 - 4k_0^2 q^2} + \varepsilon \left( 1 - \frac{1}{q^2} \right) + \frac{\alpha}{2} \right], \quad (14)$$

with  $q_0'' = 2q_0/w^2$ . In deriving this equation we made use of the equilibrium condition Eq.(B6). The eigenmode equation (13) in the case of parabolic pressure profile is the same as Eq.(29) first derived in Ref. [2], where the effect of averaged curvature (two last terms in Eq.(14)) was identified.

Qualitative analysis of the pressure gradient or finite  $\alpha$  effect on RSAEs can be done based on Eq.(14). The analysis presented here is similar to the one of Ref. [2]. The second term in the square brackets of the equation for  $Q_p$  is the only term responsible for  $\alpha$  effect in Ref. [3] and thus it is clear that an erroneous conclusion was made with regards of this effect. Indeed, that term cancels with the last term in  $Q_p$  expression ( $\alpha/2$ ), precisely at the minimum of the frequency chirp, i.e. when  $|\bar{\omega}_0| = |k_0| \ll 1/2$ . In this case the curvature driven term (third term in square brackets) leads to the upshift of the RSAE eigenfrequency if  $q > 1$ . Note that this property can be used for RSAE stabilization by lowering  $q_{min}$  below one, which, however, seems not likely to be achieved experimentally.

In the case of the RSAE frequency approaching the TAE gap, i.e.  $4k_0 q \lesssim 1$ , the first two first terms in the square bracket of Eq.(14) dominate. The balance of these two terms determines the effect of the pressure gradient on the RSAE eigenfrequency below (but close to) the TAE gap, but it is sensitive to the details of the pressure profile (see Eqs(B7, B8)). Qualitatively, in this case  $Q_p \sim \Delta' - \alpha/2$  helps to form the potential well for the RSAE for small  $\alpha$  and stabilizes the RSAE for large  $\alpha$ . However strictly speaking the analysis we have performed is not applicable at the TAE gap frequency because two harmonics,  $m$  and  $m - 1$ , become comparable.

### III. NUMERICAL STUDY OF THE PRESSURE GRADIENT EFFECT ON RSAE AND COMPARISON WITH THEORIES

#### A. Existing approximate analytical solutions vs NOVA simulations

The dispersion of equation (13) was given in [8, 14] based on matching appropriate solutions at different regions for  $|Q - 1/4| \ll 1$  case

$$S_\omega = C^2 e^{-2l\pi/\sqrt{Q-1/4}}, \quad (15)$$

where,  $C = 43.2$  and  $l$  is positive integer index of the mode radial number. In the opposite case  $|Q - 1/4| \gg 1$  the dispersion was obtained as

$$S_\omega = Q - (2l - 1) \sqrt{Q}, \quad (16)$$

with lowest solution corresponding to  $l = 1$ . Both Eqs.(15,16) have rather limited practical application.

In Figure 1 we show the comparison of exact RSAE system solution from NOVA with different analytical solutions for an  $n = 10$  mode. We chose basic plasma parameters corresponding to the tokamak ordering  $R_0 = 10m$ ,  $R/a = 10$ ,  $q_{min} = 1.98$  at  $r/a = 0.5$ ,  $\beta_0 = 0.1\%$ , parabolic pressure profile, constant density profile,  $v_A/2\pi R_0 = 233.5kHz$ , and  $\omega_{TAE} = 2\pi 58.3rad/sec$  (at  $q = 2$ ). Figure 1 (a) shows the difference between the continuum and the RSAE eigenfrequency with the continuum frequency  $23.6kHz$ . The NOVA-K code is able to compute the continuum damping in a perturbative manner [15]. The continuum damping of RSAE computed using NOVA-K is given in Fig. 1 (b).

As expected Eq.(15) gives the correct dispersion near one point on the graph, i.e. at  $Q = 1/4$ , which corresponds to  $w = 0.8$ . It quickly diverges from the RSAE eigenfrequency as  $Q$  increases. It is interesting that NOVA shows strong continuum damping for  $w < 1.15$  ( $Q < 0.5$ ), i.e. when the eigenfrequency from the dispersion relation Eq.(15) in Fig.1(a) (curve 1) is in agreement with numerical simulations. The strong increase of the damping near  $w = 1$  is due to the RSAE intersection with the continuum causing strong interaction with the continuum and strong damping. Such high values of the continuum damping mean that the perturbation method can not be applied, but it is also clear that the RSAE mode is strongly damped and thus RSAEs are likely to be stable. Curve 2 in Fig. 1 (a) (as was claimed in [8]) only asymptotically approaches the numerical eigenfrequency, that is

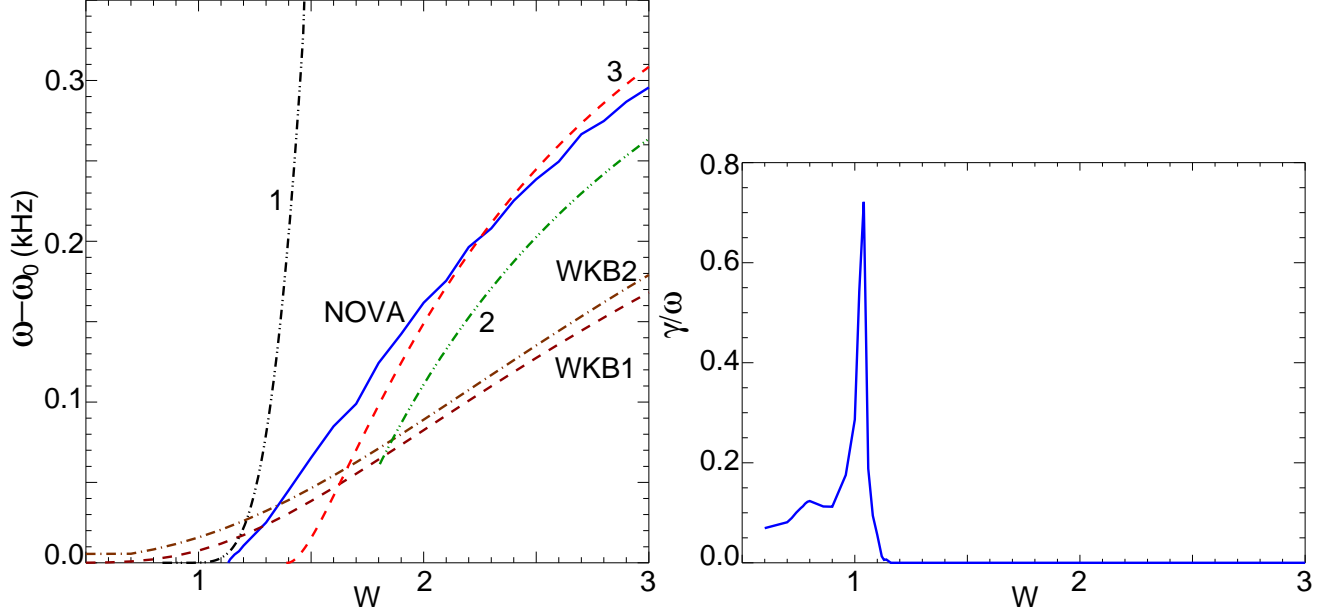


Figure 1: (a) Comparison of different RSAE eigenfrequencies for analytical solutions of the eigenmode equation (13) with the NOVA predictions for tokamak ordering equilibrium at high aspect ratio versus the characteristic width of the  $q$ -profile as defined in Eq.(B1).  $\omega_0$  is the continuum frequency at  $q = q_{min}$  surface. (b) Shows the NOVA computed continuum damping. Shown in figure (a) are predictions of NOVA as indicated, Eq.(15) - curve 1, Eq.(16) - curve 2, Eq.(20) - curve WKB2, numerical evaluation of WKB dispersion Eq.(18) - curve WKB1, and variational principle method Eq.(25) at  $p = 2$  - curve 3.

for  $Q \gg 1$ . In the plasma scenario we have chosen there is a noticeable difference with numerical simulations even for  $w > 3$ , in which case, however, the  $q$  profile is already very flat which is not relevant to typical experimental conditions.

## B. WKB dispersion

We now explore other approximate solutions to the RSAE equation. Applying the WKB technique to Eq.(13) using the ansatz  $\phi_0 = \phi_{0k} \exp(-i \int^x k_x dx)$  with the additional assumptions

$$|\partial \ln \phi_{0k} / \partial x|, |\partial \ln k_x / \partial x| \ll |k_x|, \quad (17)$$

Eq.(13) can be transformed into

$$k_x^2 = \frac{Q}{S_\omega + x^2} - 1. \quad (18)$$

The solution is localized within  $x = \pm x_c \equiv \pm\sqrt{Q - S_\omega}$  and the quantization condition provides the eigenmode dispersion  $\int k_x dx = l\pi$ , where the integral should be taken in the region of positive  $k_x$ . We present this dispersion by introducing a new radial variable  $x' = x/x_c$ :

$$x_c \int_{-1}^1 k_x dx' = \frac{2}{\sqrt{S_\omega}} \left( QK \left( i \frac{x_c}{\sqrt{S_\omega}} \right) - S_\omega E \left( i \frac{x_c}{\sqrt{S_\omega}} \right) \right) = l\pi, \quad (19)$$

where  $K$  and  $E$  are full elliptic integrals of the first and second kind, respectively. This dispersion relation can be written approximately as

$$2lS_\omega^p = (Q - S_\omega)^{p+1/2}, \quad (20)$$

where we have made use of the approximation  $4[K(iz)(z^2 + 1) - E(iz)] = \pi z^{2p+1}$ , valid for  $1 < \sqrt{z} < 10$  and  $p = 1/3$  and for  $\sqrt{z} < 1$  and  $p = 1/2$ , which covers the range of typical parameters in experiments.

As one can see from Figure 1 (a) the WKB analytical dispersion (curve WKB2), Eq.(20), is close to an accurate integration of Eq.(18) (curve WKB1) and provides reasonable connection between curves 1 and 2, but diverge from the NOVA frequency otherwise. The disagreement is mostly because the conditions for the validity of Eq.(17) are not met, as the expression for  $k_x$  varies strongly at the boundaries of the localization region.

### C. Variational principle RSAE solution

In this method we use the following ansatz for the solution

$$\phi_0 = e_0 \exp(-|x/\delta|^p / 2). \quad (21)$$

Substituting Eq.(21) into Eq.(13), multiplying by  $\phi_0$  and integrating over  $x$  we obtain the following quadratic form or Lagrangian functional

$$L = \frac{-e_0^2}{4pA\delta} \left( 4\delta^4 \Gamma \left( \frac{3}{p} \right) A + S_\omega A \Gamma \left( \frac{p-1}{p} \right) p(p-1) + \delta^2 \pi (1+p-4(Q-S_\omega)) \right), \quad (22)$$

where  $A = \Gamma((p-1)/p) \sin(\pi(p-1)/p)$ . Taking its variation with respect to  $\delta$  we find

$$12\delta^4 \Gamma\left(\frac{3}{p}\right) A + \delta^2 \pi (1 + p - 4(Q - S_\omega)) - S_\omega A \Gamma\left(\frac{p-1}{p}\right) p(p-1) = 0, \quad (23)$$

where the positive root of  $\delta^2 = \delta_2^2$  should be taken, which corresponds to the local maximum of the quadratic form. Finally, we obtain the RSAE dispersion relation by varying  $L$  over  $e_0$  and taking into account Eq.(23) to derive two equations:

$$S_\omega = 4\delta_2^4 \Gamma\left(\frac{3}{p}\right) / \Gamma\left(\frac{2p-1}{p}\right) p^2. \quad (24)$$

and

$$S_\omega = \pi^2 (Q - S_\omega - (1+p)/4)^2 / 4\Gamma\left(\frac{3}{p}\right) A^2 \Gamma\left(\frac{2p-1}{p}\right) p^2. \quad (25)$$

Note that  $p$  can be readily obtained as a function of  $S_\omega, Q, \delta$  by making use of the same variational technique. However we prefer to keep it as a parameter because the formulation can become less transparent for the analysis. It can be shown, though, that near the threshold of the RSAE existence condition, i.e.  $S_\omega = 0$ , both  $p$  and  $\delta$  tends to go to zero (with appropriate proportionality coefficient). It follows from Eq.(25), then, that  $Q > 1/4$  is the condition for  $S_\omega$  to be positive, i.e. the condition for the RSAE to be above the continuum. This coincides with the criteria derived in [8].

One can make a useful observation from Eq.(24) on the characteristic width of the RSAE radial structure. Wavevector can be defined in this case as  $k_x^2 \equiv -(\partial^2 \phi_0 / \partial^2 x) / \phi_0$  we find that  $k_x = \delta^{-1} = S_\omega^{-1/4} \left(4\Gamma\left(\frac{3}{p}\right) / \Gamma\left(\frac{2p-1}{p}\right) p^2\right)^{1/4}$ . Since  $k_x = \partial_r / m$  is the ratio of radial wavevector to poloidal one we conclude that RSAE local wavevector is in radial direction if  $k_x > 1$  or  $S_\omega \ll 1$  and in poloidal direction in opposite case  $S_\omega \gg 1$ .

In Figure 1 the variational principle based solution for  $p = 2$  fits best the NOVA RSAE frequency dependence. This is because we did not approximate the effective potential for the solution as is done in Ref.[8], but rather adjusted parameters in the chosen ansatz for the unknown solution and kept the exact potential. Lowering  $p$  helps to fit the numerical solution only at near threshold both in mode frequency and in mode structure, which is in agreement with NOVA findings.

Figure 2 shows a comparison of the RSAE radial structure of its electrostatic potential from NOVA and its variational principle solution for the plasma considered earlier with  $w = 2, \beta_0 = 0.1\%$ . It shows that the agreement is good in the region of RSAE localization.

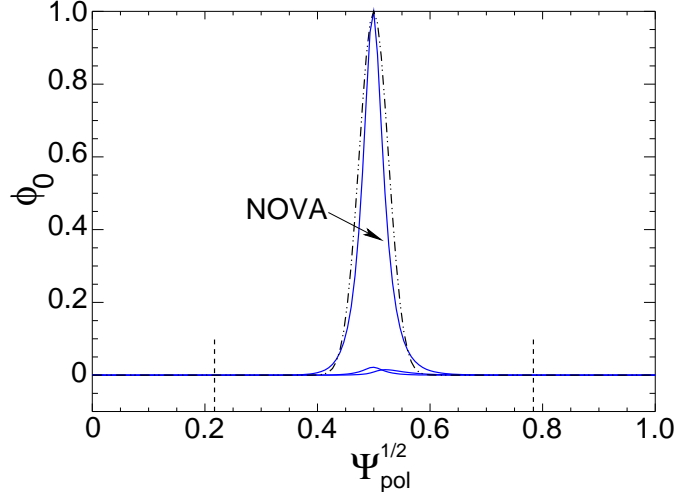


Figure 2: Variational principle solution (dot-dashed curve) comparison with the numerical NOVA solution shown as indicated solid curve. Dashed vertical lines indicate the location of the mode resonances with the continuum.

#### D. $\alpha$ dependence of the RSAE eigenfrequency beyond the tokamak ordering

It turns out that the variational principle solution is of practical interest even above the tokamak ordering limits. Let us increase the plasma pressure beyond that limit, which corresponds to the chosen basic plasma  $\alpha = 0.04$ , and compare the results with NOVA simulations. Figure 3 (a) demonstrates such a comparison, where again the variational principle solution gives the best fit to the numerical eigenfrequency.

It is important to compare our results with the earlier predictions, which is done in Fig. 3 (b). It shows how critical the effect of the pressure gradient is for the RSAE existence. For this purpose we assumed that  $S_w = Q$  for simplicity. Indeed, if the pressure gradient contribution in the second term in square brackets of expression (14) for  $Q_p$  is the only term kept, the RSAE frequency quickly decreases with  $\alpha$  and moves into the continuum, which shows its stabilizing role. The variational principle solution, on the other hand, elevates the RSAE eigenfrequency above the continuum in agreement with the NOVA calculations shown in Figs. 3 (a) and (b). We stress that this is due to the pressure gradient contribution to the Shafranov shift and to the averaged magnetic field line curvature.

It is straightforward to plot the RSAE frequency chirp predictions as  $q_{min}$  decreases (for the case of interest,  $w = 2$ ) from  $q_{min} = 2$  to  $(m - 1)/n = 1.95$  (see Figure 4). It is clear from this figure that again the variational principle solution shows the role of  $\alpha$  in determining the

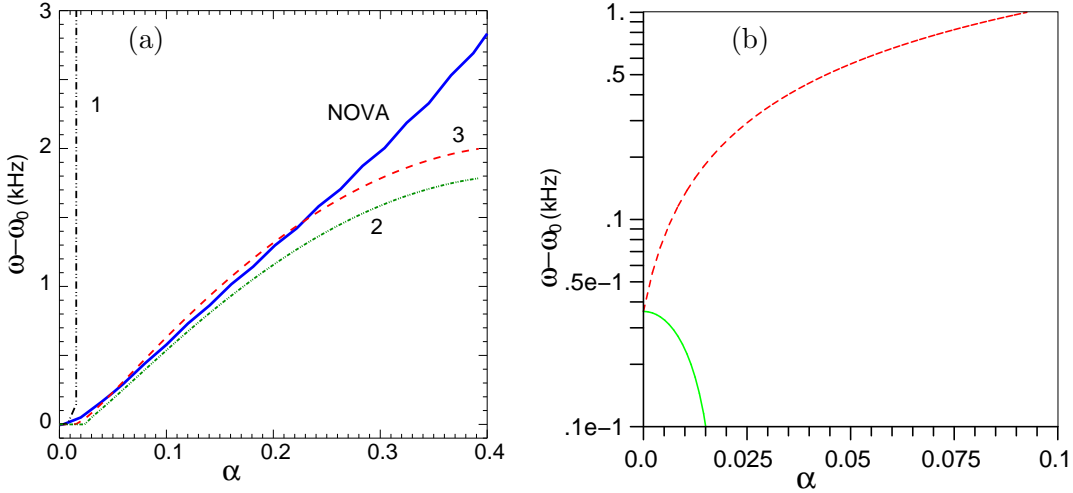


Figure 3:  $\alpha$  dependence of the RSAE eigenfrequency for  $w = 2$ . In figure (a) analytical solutions are denoted the same way as in Figure 1. For the comparison  $Q \simeq 1/4$  at  $\alpha = 0$  in this plot and reaches  $Q = 5.5$  at  $\alpha = 0.2$ . (b) Shows the comparison of the variational principle solution (dashed curve) with the dispersion relation prediction from Ref. [3] (solid curve).

mode frequency upshift at the lower part of the chirp, but becomes stabilizing at the high end of the mode chirp, whereas the expression given in Ref.[3] predicts strong stabilization of the mode due to the  $\alpha$  effect. In the latter case the contribution from fast ions to  $Q$  [8] has to be invoked to account for the mode existence in experiments. We note however that recent studies show good agreement between NOVA simulated RSAE eigenfrequencies and experimental measurements [16]. More detailed studies to separate the ideal MHD and fast ion contributions to  $Q$  should be done in the future.

#### IV. IMPLICATIONS FOR MHD SPECTROSCOPY

In the past it was shown that the RSAE frequency can be used as an accurate diagnostic of  $q_{min}$  [8]. It has recently been argued that the minimum frequency of the RSAE during the cycle of chirping can also be used to diagnose the plasma pressure [3], where it was stated that  $\omega_{min} = c_s R_0^{-1} (2 + q^{-2})$ , with  $c_s$  the sound speed, which in MHD theory is proportional to the total plasma beta  $c_s \sim \gamma \beta_{pl}$ . With the results obtained in the present paper we conclude that the minimum frequency is determined not only by the finite plasma pressure

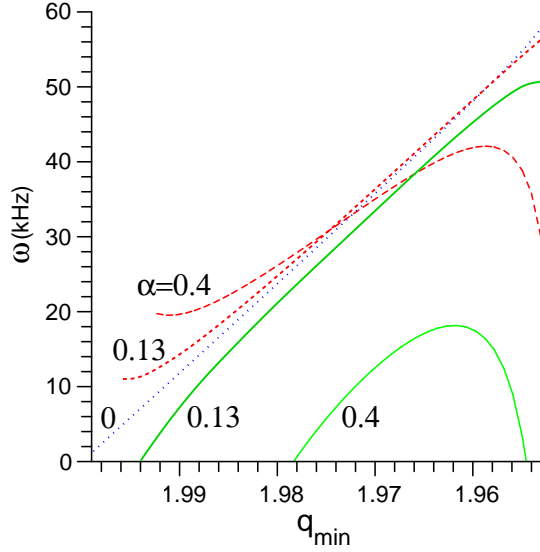


Figure 4: Predictions for the frequency chirp of RSAE mode versus  $q_{min}$  for variational principle solution given by Eq.(25) and shown as dashed lines, and dispersion relation from Ref. [3] (solid curves) for different values of  $\alpha$ . Shown as dotted curve at  $\alpha = 0$  is the RSAE frequency, for which both model give the same mode frequency, which closely follows the continuum. On this plot TAE frequency at  $q_{min} = 1.95$  corresponds to  $\omega_{TAE} = 59kHz$ .

but also by its gradient. Thus the diagnostic application of RSAE theory predictions as it was postulated in Ref.[3] should work only for plasmas with zero pressure gradient and needs revision for realistic plasmas.

Without additional information about the pressure gradient it is not possible to make use of the  $\omega_{min}$  for diagnostic purposes. However, such information can be obtained by measuring the frequency separation between RSAEs at the same  $m$  and  $n$  numbers but with different  $l$  radial numbers, such as in dispersions Eqs.(15) and (16). For better accuracy we extend the variational method for fixed  $p = 2$  (see Eq.(21)) by multiplying the ansatz function by the Hermite polynomials and, thus, constructing the following ansatz

$$\phi_0 = e_0 \exp \left[ - (x/\delta)^2 / 2 \right] H_{l-1} (x/\delta). \quad (26)$$

Similar to section III C we find

$$L = \frac{e_0^2 2^{l-1} (l-1)! \sqrt{\pi}}{\delta} \left[ \left( \frac{l(l-1)}{2} + \frac{3}{4} + S_w - Q \right) \delta^2 + (S_w + \delta^4) \left( l - \frac{1}{2} \right) \right]. \quad (27)$$

Taking variation of this form with respect to  $\delta$  we find

$$6\delta^4(2l-1) + 4\delta^2 \left( S_\omega - Q + \frac{l(l-1)}{2} + 3/4 \right) - 2S_\omega(2l-1) = 0.$$

Finally the dispersion relation is reduced to the form  $S_\omega = \delta^4$ , which we rewrite as a quadratic equation

$$\sqrt{S_\omega} = \frac{Q - S_\omega - l(l-1)/2 - 3/4}{2l-1}, \quad (28)$$

which appropriate solution is

$$S_\omega = Q - \sqrt{2}\sqrt{2Q + l^2 - l - 1} \left( l - \frac{1}{2} \right) + \frac{3}{2} \left( l^2 - l - \frac{1}{6} \right).$$

The RSAE dispersion, Eq.(28), at  $l = 1$  is the same as Eq.(25) at  $p = 2$  and is plotted as curve 3 in figures 1 (a) and 3 (a). It shows the best agreement with NOVA computations over a wide range of plasma parameters.

It is straightforward then to obtain the value of  $\alpha$  from expressions (14) and (28) or from numerical NOVA modeling, when changing  $l$ . Then, at a given  $l$  and  $\alpha$  one can find the frequency shift from the continuum and deduce it from the experimentally observed RSAE frequency in order to find the GAM shift and thus the sound speed of the plasma. We note that with the theory we present this diagnostic application can be done only for  $\omega > \omega_{min}$  as it breaks down for  $\omega = \omega_{min}$  due to  $k_0 = 0$ .

## V. DISCUSSION AND CONCLUSIONS

We have shown both analytically and numerically that the pressure gradient is responsible for an upshift of the RSAE frequency (at fixed  $q_{min}$ ) in the low frequency range of the chirp. It is also responsible for the frequency downshift when the mode begins to transition to the TAE gap, i.e. near the top of RSAE frequency range (this is qualitatively similar to prediction made in Ref. [9]). These results confirm the numerical findings of Ref. [1] and analytical insight on the role of pressure gradient first obtained in Ref. [2]. We also showed that in realistic plasma conditions the pressure gradient can play a dominant role for the existence of the RSAEs. This is due to the pressure gradient contribution to the Shafranov shift and due to the averaged magnetic field line curvature effect. As an ingredient of  $\omega_{min}$ , the minimum frequency of the RSAE chirp, the pressure gradient effect can compete with the finite pressure effect pointed out in Ref. [3] (see also Ref.[10]).

We have improved the analytical dispersion relation by applying the variational principle technique to the RSAE eigenmode equation. The obtained eigenfrequency and RSAE mode structure are in a good agreement with NOVA over a wide range of plasma parameters, even beyond the tokamak ordering of low beta. With this new variational principle dispersion relation we clearly demonstrate the diagnostic potential and limitations of the RSAE frequency measurement for MHD spectroscopy.

Realistic simulations should be performed with numerical tools as the continuum itself is strongly affected by the pressure gradient. For investigation of experimental results as well as the verification and validation of analytical theories it seems critical to make use of established, validated, and widely available codes such as MISHKA [17], CASTOR [18], and NOVA [4, 5]. Application of such codes should help to distinguish the role of ideal MHD effects from fast ion effects in driving and/or creating conditions for the existence of RSAEs.

### **Acknowledgments**

We are also grateful to Dr. G.Y. Fu for making available the draft of the paper [2] prior to its submission and for discussions on the role of the averaged curvature term.

This work was supported by the United States Department of Energy under Contract No. DE-AC02-76CH03073.

### **Appendix A: EQUILIBRIUM GEOMETRY AND MODEL PLASMA PROFILES**

The analytical derivations are performed in a low- $\beta$  plasma equilibrium [11, 19]. The magnitude of the equilibrium magnetic field is given by  $B = B_0 (1 - \beta(r)/2 - (r^2 - 2a^2)/2q^2R_0^2)/R$ , where  $B_0$  is the vacuum magnetic field at the plasma axis and we assume that the magnetic shear is low at the point of interest. We also note that  $g = B_\phi R = B_0 (1 - \beta(r)/2 - (r^2 - a^2)/q^2R_0^2)$ , where  $\beta$  is the ratio of the plasma pressure to the magnetic field pressure.

The flux function  $\psi$  depends on the minor radius only and is related to the minor radius according to  $\psi' = g\varepsilon/q$ . The Shafranov shift corresponding to the pressure profiles, Eqs.(B2,B3), is calculated in Appendix B, for which to be valid one has to assume the

so-called tokamak ordering,  $\alpha = O(\varepsilon)$  and  $\beta = O(\varepsilon^2)$ . We will show that for higher beta the numerical solution of MHD equations is required. For the low- $\beta$  plasma and equal arc poloidal angle it was found [11] that the Jacobian is  $\mathcal{J} = ([\nabla r \times \nabla \theta] \cdot \nabla \varphi)^{-1} = rR_0(1 + (\varepsilon - \Delta') \cos \theta)$ , and  $\nabla r \cdot \nabla r = 1 + 2\Delta' \cos \theta$ ,  $\nabla r \cdot \nabla \theta = \Delta' r^{-1} \sin \theta$ ,  $\nabla \theta \cdot \nabla \theta = r^{-2}$ ,  $\nabla \varphi \cdot \nabla \varphi = R^{-2} = R_0^{-2}(1 - 2\varepsilon \cos \theta)$ . We note the following useful relations

$$\frac{\mathbf{B} \times \nabla \psi}{B^2} \cdot \nabla = \frac{g^2 \varepsilon}{\mathcal{J} q B^2} \frac{\partial}{\partial \theta}, \quad (\text{A1})$$

$$\frac{\nabla \psi \cdot \nabla}{|\nabla \psi| |\nabla r|} = \frac{\partial}{\partial r} - \frac{\sin \theta (\Delta' + r \Delta'' + \varepsilon)}{r} \frac{\partial}{\partial \theta}, \quad (\text{A2})$$

$$\mathbf{B} \cdot \nabla = \frac{g\varepsilon}{J} \partial_{\parallel} \equiv \frac{g\varepsilon}{Jq} \left( q \frac{\partial}{\partial \zeta} + \frac{\partial}{\partial \theta} \right). \quad (\text{A3})$$

Note, that operating on the perturbed quantities, (Eq.(8)), we define the parallel wavevector through

$$\left( e^{-i(m\theta + j\theta - n\zeta)} \partial_{\parallel} \phi_j e^{i(m\theta + j\theta - n\zeta)} \right) = ik_j \phi_j = i(m + j - nq) \phi_j / q = i(k_0 + j/q) \phi_j. \quad (\text{A4})$$

Local negative shear,  $S$ , is introduced through the following expression

$$|\nabla \psi|^2 S \equiv (\mathbf{B} \times \nabla \psi) \cdot \nabla \times \frac{\mathbf{B} \times \nabla \psi}{|\nabla \psi|^2} = \frac{|\nabla r|^3 g^2}{R^3 q} [-s + (r \Delta'' + \Delta' + \varepsilon) \cos \theta], \quad (\text{A5})$$

where  $s = rq'/q$ . Equilibrium plasma current is included in the equation in the following combination

$$BJ_{\parallel} - |\nabla \psi|^2 S = -R^{-2} \nabla g \cdot \nabla \psi + g \nabla (R^{-2} \nabla \psi) - |\nabla \psi|^2 S = \frac{2g^2}{R_0^3 q} (1 + (\Delta' - 3\varepsilon) \cos \theta) \quad (\text{A6})$$

Curvature components are given via:

$$\begin{aligned} k_{\psi} &\equiv 2 \nabla \psi \cdot \mathbf{k} = B^{-2} \nabla \psi \cdot \nabla (2P + B^2), \\ k_s &\equiv 2B^{-2} (\mathbf{B} \times \nabla \psi) \cdot \mathbf{k} = B^{-4} (\mathbf{B} \times \nabla \psi) \cdot \nabla B^2. \end{aligned}$$

Using the tokamak ordering we find

$$\begin{aligned} k_{\psi} &= 2\varepsilon g (1 + 2\Delta' \cos \theta) q^{-1} R^{-1} \left[ \Delta' - \cos \theta - \frac{\varepsilon}{q^2} - \Delta' \sin^2 \theta \right], \\ k_s &= 2g^2 \varepsilon r \sin \theta / B^2 \mathcal{J} q R. \end{aligned} \quad (\text{A7})$$

## Appendix B: SHAFRANOV SHIFT FOR NON-CONSTANT CURRENT DENSITY PROFILE

We define the plasma safety factor profile in the form

$$q = q(r) = q_{min} / (1 - (r - r_0)^2 / w^2), \quad (\text{B1})$$

where  $q_{min}$  is the minimum of the safety factor at  $r = r_0$ ,  $r$  is the square root of the normalized toroidal flux, and  $w$  is the characteristic width. Two different pressure profile will be used, linear:

$$\beta = \beta_0 (1 - r/a), \quad (\text{B2})$$

and parabolic:

$$\beta = \beta_0 (1 - (r/a)^2). \quad (\text{B3})$$

Equation for the Shafranov shift, defined through  $R = R_0 - \Delta + r \cos \theta$ , is:

$$\frac{d}{dr} (r B_\theta^2 \Delta') = \frac{r}{R_0} \left( -B_\varphi^2 r \frac{d\beta}{dr} + B_\theta^2 \right), \quad (\text{B4})$$

where  $\Delta' \equiv d\Delta/dr$ ,  $R_0$  is the magnetic axis radius. Integrating Eq.(B4) from the center to  $r$ , we find:

$$\Delta' = \frac{R_0 q^2}{r} \left( r^{-2} \int_0^r \beta dr^2 - \beta \right) + \frac{q^2}{R_0 r^3} \left( \int_0^r \frac{r^3}{q^2} dr \right). \quad (\text{B5})$$

It also follows from Eq.(B4) that to the lowest order in  $\varepsilon$

$$3\Delta' + r\Delta'' = \varepsilon + \alpha. \quad (\text{B6})$$

For a constant pressure profile the first term in Eq.(B5) is zero and we obtain in the vicinity of  $r = r_0$ :

$$\Delta'_0 \equiv \frac{q^2}{R_0 r^3} \left( \int_0^r \frac{r^3}{q^2} dr \right) \simeq \frac{r}{4R_0} - \left( \frac{2r_0}{15} - \frac{r}{10} \right) \frac{r_0^2}{w^2 R_0},$$

where we neglected terms with small coefficients to simplify the analytical treatment, which may change the result by  $\sim 1\%$ . In the limit of a flat current profile, i.e.  $w \rightarrow \infty$ , the above expression is reduced to well known limit  $\Delta'_0 = r/4R_0$ . For a linear pressure profile using Eq.(B2), we find

$$\Delta' = \frac{R_0 q_0^2}{3a} \beta_0 + \Delta'_0 = \frac{\alpha}{3} + \Delta'_0, \quad (\text{B7})$$

where  $\alpha \equiv -R_0 q^2 \beta'$ . For a parabolic pressure profile, Eq.(B3), we find

$$\Delta' = \frac{R_0^2 q_0^2}{2a^2} \beta_0 \varepsilon + \Delta'_0 = \frac{\alpha}{4} + \Delta'_0. \quad (\text{B8})$$

We note that  $O(\beta) = \varepsilon O(\alpha)$  and that for a linear pressure profile  $\alpha = \text{const}$ , whereas for a parabolic profile  $\alpha \sim r$ .

- 
- [1] G. J. Kramer, N. N. Gorelenkov, R. Nazikian, and C. Z. Cheng. Finite pressure effects on reversed shear Alfvén eigenmodes. *Plasma Phys. Contr. Fusion*, 46:L23–L29, September 2004.
  - [2] G. Y. Fu and H. L. Berk. Effects of pressure gradient on existence of Alfvén cascade modes in reversed shear tokamak plasmas. *Phys. Plasmas*, 13:052502–1–052502–6, May 2006.
  - [3] B. N. Breizman, S. E. Sharapov, and M. S. Pekker. Plasma pressure effect on Alfvén cascade eigenmodes. *Phys. Plasmas*, 12:112506–1–112506–9, December 2005.
  - [4] C. Z. Cheng and M. S. Chance. Low-n shear Alfvén spectra in axisymmetric toroidal plasmas. *Phys. Fluids*, 29:3695–3701, November 1986.
  - [5] C. Z. Cheng. Kinetic extensions of magnetohydrodynamics for axisymmetric toroidal plasmas. *Phys. Reports*, 211:1–51, January 1992.
  - [6] S. E. Sharapov, B. Alper, H. L. Berk, D. N. Borba, and et. al. Alfvén wave cascades in a tokamak. *Phys. Plasmas*, 9:2027–2036, May 2002.
  - [7] R. Nazikian, B. Alper, H. L. Berk, D. Borba, and et.al. Observation of energetic particle driven modes relevant to advanced tokamak regimes. *in Proceedings of 20th IAEA Fusion Energy Conference, Vilamoura, Portugal*), IAEA-CN-116/EX/5-1:1–9, November 2004.
  - [8] H. L. Berk, D. N. Borba, B. N. Breizman, S. D. Pinches, and S. E. Sharapov. Theoretical interpretation of Alfvén cascades in tokamaks with nonmonotonic  $q$  profiles. *Phys. Rev. Letters*, 87:185002–1–185002–4, October 2001.
  - [9] G. Y. Fu. Existence of core localized toroidicity-induced Alfvén eigenmode. *Phys. Plasmas*, 2:1029–1031, April 1995.
  - [10] M. S. Chu, J. M. Greene, L. L. Lao, A. D. Turnbull, and M. S. Chance. A numerical study of the high-n shear Alfvén spectrum gap and the high-n gap mode. *Phys. Fluids B*, 11:3713–3721, November 1992.
  - [11] J. M. Greene, J. L. Johnson, and K. E. Weimer. Tokamak equilibrium. *Phys. Fluids*, 14:671–683, March 1971.
  - [12] B. N. Breizman, H. L. Berk, M. S. Pekker, S. D. Pinches, and S. E. Sharapov. Theory of Alfvén eigenmodes in shear reversed plasmas. *Phys. Plasmas*, 10:3649–3660, September 2003.

- [13] S. V. Konovalov, A. B. Mikhailovskii, M. S. Shirokov, E. A. Kovalishen, and T. Ozeki. Kinetic reversed-shear Alfvén eigenmodes. *Phys. Plasmas*, 11:4531–4534, September 2004.
- [14] S. E. Sharapov, A. B. Mikhailovskii, and G. T. A. Huysmans. Effects of nonresonant hot ions with large orbits on Alfvén cascades and on magnetohydrodynamic instabilities in tokamaks. *Phys. Plasmas*, 11:2286–2302, May 2004.
- [15] N. N. Gorelenkov. Double-gap Alfvén eigenmodes: Revisiting eigenmode interaction with the Alfvén continuum. *Phys. Rev. Letters*, 95:265003–1–265003e–4, December 2005.
- [16] G. J. Kramer, R. Nazikian, B. Alper, M. de Baar, and et. al. Interpretation of core localized Alfvén eigenmodes in diii-d and joing european torus reversed magnetic shear plasmas. *Phys. Plasmas*, 13:056104–1–056104–7, May 2006.
- [17] G. T. A. Huysmans, S. E. Sharapov, A. B. Mikhailovskii, and W. Kerner. *Phys. Plasmas*, 8:4292–4300, September?? 2001.
- [18] W. Kerner, J. P. Goedbloed, G. T. A. Huysmans, S. Poedts, and E. Schwartz. *J. Comput. Phys.*, 142:271–281, 1998.
- [19] Roscoe B. White. *The Theory of Toroidally Confined Plasmas*. Imperial College Press, London, UK, second edition, 2001.
- [20] A sign error in our original derivation of the terms responsible for the numerically observed pressure gradient effect (pointed out by S. Sharapov in private communication, 2004) did not affect the validity of our original interpretation [1].

The Princeton Plasma Physics Laboratory is operated  
by Princeton University under contract  
with the U.S. Department of Energy.

Information Services  
Princeton Plasma Physics Laboratory  
P.O. Box 451  
Princeton, NJ 08543

Phone: 609-243-2750  
Fax: 609-243-2751  
e-mail: [pppl\\_info@pppl.gov](mailto:pppl_info@pppl.gov)  
Internet Address: <http://www.pppl.gov>